THE JOURNAL OF PHYSICAL CHEMISTRY A

Article

pubs.acs.org/JPCA

Helical Structure and Circular Dichroism Spectra of DNA: A Theoretical Study

Tomoo Miyahara,[†] Hiroshi Nakatsuji,*[,†] and Hiroshi Sugiyama[‡]

[†]Quantum Chemistry Research Institute, JST, CREST, Kyodai Katsura Venture Plaza, North Building 107, 1-36 Goryo-Oohara, Nishikyo-ku, Kyoto 615-8245, Japan

[‡]Department of Chemistry, Graduate School of Science, Kyoto University, Kitashirakawa-Oiwakecho, Sakyo-Ku, Kyoto 606-8502, Japan

Supporting Information

ABSTRACT: The helical structure is experimentally determined by circular dichroism (CD) spectra. The sign and shape of the CD spectra are different between B-DNA with a right-handed double-helical structure and Z-DNA with a left-handed double-helical structure. In particular, the sign at around 295 nm in CD spectra is positive for B-DNA, which is opposite to that of Z-DNA. However, it is difficult to determine the helical structure from the UV absorption spectra. Three important factors that affect the CD spectra of DNA are (1) the conformation of dG monomer, (2) the hydrogen-bonding interaction between two helices, and (3) the stacking interaction between nucleic acid bases. We calculated the CD spectra of (1) the dG monomer at different conformations, (2) the composite of dG and dC monomers, (3) two dimer models that simulate separately the hydrogen-bonding interaction and the stacking interaction, and (4) the tetramer model that includes both hydrogen-bonding and stacking interactions simultaneously. The helical structure of DNA can be clarified by a comparison of the experimental and SAC-CI theoretical CD spectra of DNA and that the sign at around 295 nm of the CD spectra of Z-DNA reflects from the strong stacking interaction characteristic of its helical structure.

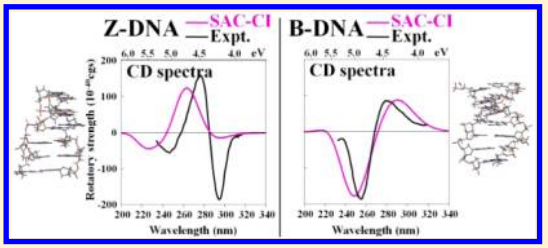

1. INTRODUCTION

All living organisms carry genetic information.[1] Eukaryotic organisms store the genetic information in the DNA in the cell nucleus. DNA is a polymer composed of purine or pyrimidine bases, deoxyriboses, and phosphate groups and forms a characteristic helical structure. DNA can exist in many different conformations.[2] In solution, the most common forms, A- and B-DNA, have right-handed double-helical structure, while Z-DNA is left-handed and appears only when DNA has a special sequence. The transition from B- to Z-DNA or from Z- to B-DNA can be induced by changes in the buffer concentration or the temperature.[3−8] DNA is a complex dynamic system and flexible in solution. It is difficult to make a simple model for DNA in solution, and also, it is difficult to analyze the transition processes from B- to Z-DNA. So, basic questions may arise: Is it possible to use a simple model to study DNA in solution? Can we understand the important aspects of DNA from the calculations using such a small simple model?

Circular dichroism (CD) spectroscopy is widely used to study the helical structure of DNA in solution.[9] The experimental ultraviolet (UV) spectra are similar between B- and Z-DNA because the electronic excitations of DNA are mainly intramolecular excitations within the nucleic acid bases. However, the experimental circular dichroism (CD) spectra of B- and Z-DNA are very different, even when the B- and Z-DNA are composed of the same sequences of nucleotides.[4−8] These differences appear even in the CD spectra of a DNA sequence composed of only six base pairs. The sign of the CD spectrum is used to identify the helical structure of DNA. However, only a few theoretical studies have investigated why the sign of the CD spectrum of DNA changes depending on the type of its helical structure. The time-dependent density functional theory (TDDFT)[10,11] was applied to the UV spectra of the DNA bases[12,13] and to the CD spectra of double-helical DNA using adenine-thymine dimer models to distinguish cross-strand base pairs and Watson−Crick base pairs[14] and of single-strand DNA using adenine dimer and tetramer to validate the structure of molecular dynamics calculations.[15] However, the TDDFT has some serious problems in Rydberg excitations,[16] in charge transfer excitations,[17] in double excitations,[18] etc. In addition, the TDDFT calculations of the CD spectra did not show sufficient accuracy.[19] To overcome these problems, the improvement of TDDFT were done.[20,21] For example, the long-range corrected (LC)-TDDFT theory[22,23] improved some of these problems but not the problems of the CD spectra. However, the symmetry-adapted cluster (SAC)-configuration interaction (CI) theory[24−27] has been applied to many different systems and gave highly reliable results for the excited states of many different types and properties[28,29] including the CD spectra.[30] This is so as long as proper active space and proper

Received: August 29, 2012
Revised: December 10, 2012
Published: December 12, 2012

   dx.doi.org/10.1021/jp3085556 | J. Phys. Chem. A 2013, 117, 42−55

basis sets are used. Actually, the SAC-CI method was used as the reference data for confirming the accuracy of the LC-TDDFT method.[22,23]

Actually, it is difficult to model DNA in solution because DNA is a complex dynamic system. However, when we use a small DNA system whose UV and CD spectra are well studied experimentally, it would be possible to calculate the UV and CD spectra of such DNA in high accuracy by the SAC-CI method, and by comparing with the experimental data, we would be able to elucidate some basic aspects of the complex phenomena. In this article, we study the UV and CD spectra of DNA and their relationships to the helical structures, using the small models taken from B- and Z-DNA composed of the same sequence of only six deoxyguanosine (dG) and deoxycytidine (dC). We want to show that even such a small model can clarify some aspects of the relationships between the CD spectra and the helical structure of DNA, when we use a highly reliable computational method like the SAC-CI method.

The difference between B- and Z-DNA is the helical-structure as well as the conformation of dG. The purine base dG has the anti conformation in B-DNA, while it has syn conformation in Z-DNA.[3] The *anti*- and *syn*-dG differ in the dihedral angle between the guanine of the purine base and deoxyribose by approximately 180°. However, the pyrimidine base dC exists as only the anti conformation in both B- and Z-DNA because of the steric hindrance between the pyrimidine base cytosine and deoxyribose.

There are three main interactions in DNA: (1) the interaction through the bond between the nucleic acid bases and the deoxyribose; (2) hydrogen-bonding interactions between two nucleic acid bases; and (3) stacking interactions between two nucleic acid bases. Our goal is to understand the roles of these interactions in forming the helical structure and how these interactions affect the CD spectra of B- and Z-DNA.

We have applied the symmetry-adapted cluster (SAC)-configuration interaction (CI) theory[24−27] to elucidate the underlying relationships between the helical structure of DNA and the sign of their CD spectra. The SAC-CI theory is a reliable method for studying the UV and CD spectra in relation to the electronic and geometrical structures of the biological system and chiral compounds.[30−34] We calculated the UV and CD spectra of the monomer of dG in various conformations including both anti and syn conformations. For the dC monomer, however, we performed calculations only for the anti geometries observed in B- and Z-DNA because the conformation of dC is rigid in DNA. For purposes of comparison, we used an experimentally acquired spectrum of dG obtained in aqueous solution.[35] We also studied the UV and CD spectra of DNA. First, we approximated the spectra as a simple sum of the spectra of dG and dC that have the structure in B- and Z-DNA. Next, we calculated the UV and CD spectra using dimer models of B- and Z-DNA that represented either the hydrogen-bonding interaction or the stacking interactions. Finally, we calculated the UV and CD spectra using tetramer models of B- and Z-DNA that included both of the hydrogen-bonding and stacking interactions within the same model. All of the models include the through-bond interactions between the nucleic acid base and the deoxyribose.

2. MODELING AND COMPUTATIONAL DETAILS

The SAC-CI theory is a useful coupled-cluster type electron correlation theory for studying ground, excited, ionized, and electron-attached states of molecules published in 1978.[24−27] The so-called EOM-CC method published about a decade later[36,37] is very similar to the SAC-CI method, although called a different name. This equivalence was shown even numerically in the previous publications.[38,39] For the calculations of the CD spectra of large molecules, the gauge-invariant velocity form must be used since the position of the gauge origin is not known. The independence of the SAC-CI method from the gauge origin has already been determined for the three-membered ring compounds.[30]

First, we studied the dependence of the CD spectrum on the conformation of the dG monomer. The ground state geometries with both anti and syn conformations of dG were optimized with Gaussian03[40] using the density functional theory (DFT)[41−44] with the B3LYP functional[45,46] for the 6-31G(d,p) basis[47,48] sets. All of the geometrical parameters of dG except for the dihedral angle φ were optimized at every 20° in the potential energy for the ground state of dG. Full optimization was done for anti and syn conformations. The solvent effects of water were considered using the polarizable continuum model (PCM)[49] that was connected recently with the SAC-CI method in the Gaussian suite of programs.[50]

We then analyzed the UV and CD spectra of B- and Z-DNA obtained using the dimer model, which contains either the hydrogen-bonding interaction or the stacking interaction, and next using the tetramer model, which contains both the hydrogen-bonding and stacking interactions within the same model (Figure 1). The geometries were taken from the X-ray crystallography structure. 9BNA and 1DCG were used for B- and Z-DNA, respectively. In B-DNA, the GC pair *weakly* stacks with both of the lower and upper GC pairs (diamond-shaped

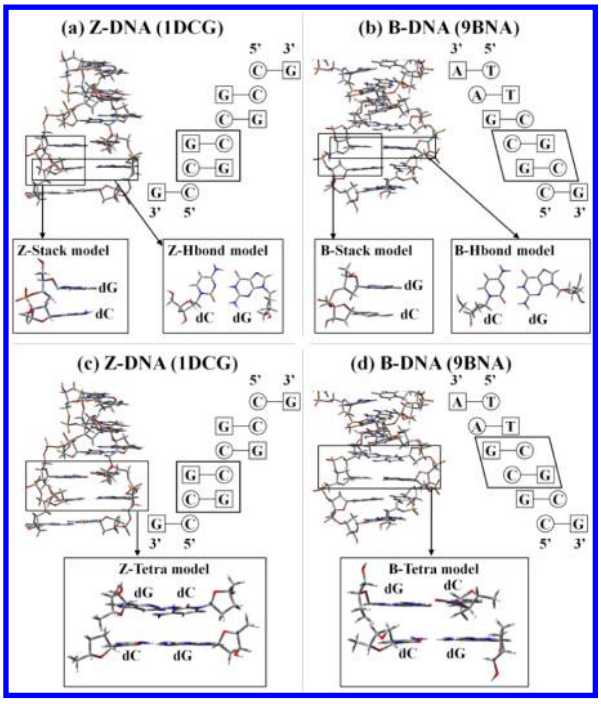

Figure 1. (a) Hydrogen-bonding (Z-Hbond) and stacking (Z-Stack) models taken from the X-ray crystallography structure (1DCG) of Z-DNA. (b) Hydrogen-bonding (B-Hbond) and stacking (B-Stack) models taken from the X-ray crystallography structure (9BNA) of B-DNA. (c) Tetramer model (Z-Tetra) taken from the X-ray crystallography structure (1DCG) of Z-DNA. (d) Tetramer model (B-Tetra) taken from the X-ray crystallography structure (9BNA) of B-DNA.

dx.doi.org/10.1021/jp3085556 | J. Phys. Chem. A 2013, 117, 42−55

box in Figure 1b,d), but in Z-DNA, the guanine-cytosine (GC) pair *strongly* stacks with only one GC pair (denoted by the square box, Figure 1a,c). The stacking model of Z-DNA (Z-Stack model) has strong stacking interactions. As in the geometry optimization for dimer and tetramer models, only the hydrogen atom positions in these models were optimized using the B3LYP/6-31G(d,p) basis with the PCM of water.

For the SAC/SAC-CI calculations, the basis functions employed were D95[51] sets for deoxyribose and D95(d)[51] sets for the nucleic acid bases. The core orbitals were treated as frozen orbitals, and all singles and selected doubles were included. Perturbation selection[52] was carried out for the double excitation operators using the threshold sets of 5×10^{-7} and 1×10^{-7} hartree for SAC and SAC-CI calculations, respectively. In the calculations for the tetramer model, the basis functions employed were D95 sets (without polarization functions) because the calculations were heavier than the calculations for the dimer model, and further, the orbitals, whose energies were within −1.1 to +1.1 au, were chosen as the active orbitals. The SAC-CI UV and CD spectra were convoluted using Gaussian envelopes to describe the Franck−Condon widths and the resolution of the spectrometer. The full width at half-maximum (fwhm) of the Gaussian was 0.8 eV, which was estimated from the criterion that the two bands (253 and 278 nm) looks like a single band in the experimental UV spectrum of dG; the lowest two bands were not divided clearly. This value (0.8 eV) was also used for the convolution of the theoretical CD spectra. Since DNA is a polymer composed of monomers, we used the same value in dimer and tetramer calculations. The UV and CD spectra of (1) dG with several conformations, (2) only dG and only dC in the X-ray crystallography structures of B- and Z-DNA, (3) the hydrogen-bonding and stacking models of B- and Z-DNA, and (4) the tetramer models of B- and Z-DNA were calculated using the SAC-CI method.

3. RESULTS AND DISCUSSION

3.1. Structure of the Ground State dG Monomer in Water. We calculated the changes in the potential energy for the ground state of the dG monomer in water as a function of changes in the dihedral angle (φ) between the deoxyribose and the guanine (Figure 2). All of the geometrical parameters of dG were optimized, and φ was varied by incremental increases of 20°. The optimized dihedral angle was calculated to be 310.3° in the anti region and at 129.5° for the syn region. The deoxyribose has C3′-endo conformation for both *anti*- and *syn*-dG with the present calculations, although for *anti*-dG, C2′-endo was calculated to be more stable than C3′-endo.[53,54] Thus, in dG, the conformation of the deoxyribose seems to be very flexible and its energy difference very small. However, the conformation of deoxyribose is rigid in DNA: the deoxyribose in dG is C2′-endo for B-DNA and C3′-endo for Z-DNA based on the X-ray crystallography structures (9BNA and 1DCG). The *anti*-dG was calculated to be more stable than the *syn*-dG by 0.47 kcal/mol. The conformation of dG converts easily from anti to syn (or from syn to anti) because the energy barrier between the anti and syn forms is only ∼5 kcal/mol. The *anti*-dG rotates more easily in the clockwise direction (the direction of the arrow in Figure 2) than in the counterclockwise direction because the energy barrier is less than 4 kcal/mol in the clockwise direction but is more than 5 kcal/mol in the counterclockwise direction. The potential energy curve is flat in the anti region, while it is sharper in the syn region because there is a hydrogen bond interaction between the hydroxyl group of the deoxyribose and the nitrogen atom of the guanine near the syn conformation. However, the *anti*-dG can rotate more freely between φ = 270° and 330° because of the lack of hydrogen-bonding interaction.

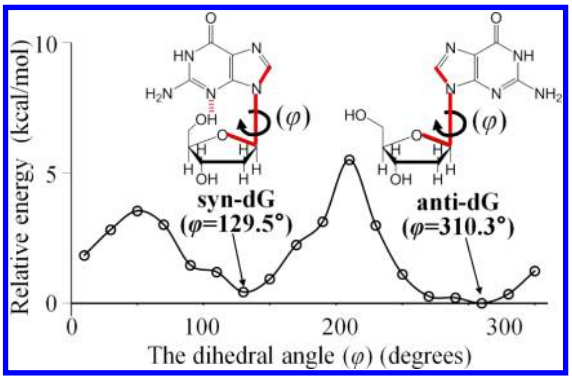

Figure 2. Potential energy curve of the ground state of dG determined as dihedral angle φ is varied in increments of 20°. Other geometrical parameters were optimized at each φ.

3.2. UV and CD Spectra of dG Monomer in Water. Using the SAC-CI method, we calculated the excitation energies, oscillator strengths, rotatory strengths, and the natures of the excited states for both of the *anti*- and *syn*-dG (Table 1). The difference in the UV excitation spectra between *anti*- and *syn*-dG is very small, within 0.07 eV in energy and within 0.08 au in oscillator strength for all the calculated states. However, for the CD spectra whose shapes are described by the rotatory strengths, the spectra of *anti*-dG differ markedly from the spectra of *syn*-dG not only in the absolute value but also in the sign of the rotatory strength. Below, we show these theoretical results in the spectral forms to facilitate the comparisons with the experimentally obtained data.

3.2.1. UV Spectra of dG Monomer. The SAC-CI UV spectra (red lines) of *anti*- and *syn*-dG were compared with the experimental spectrum (black lines) of dG above 200 nm (Figure 3). There are two main bands (276 and 250 nm) above 200 nm and one band below 200 nm. The SAC-CI UV spectra of both *anti*- and *syn*-dG are similar to the experimental UV spectrum, and therefore, it is unclear whether the experimental UV spectrum of dG is due to the anti or the syn conformation. The first band at about 276 nm was assigned to the $\pi \rightarrow \pi^*$ highest occupied molecular orbital (HOMO)−lowest unoccupied molecular orbital (LUMO) transition (1^1A state at 4.46 eV (278 nm) for *anti*-dG and 4.40 eV (282 nm) for *syn*-dG). The second band at approximately 250 nm was assigned to the 3^1A state (at 5.10 eV (243 nm) for *anti*-dG and 5.06 eV (245 nm) for *syn*-dG) of π(HOMO) → π^*(next-LUMO) and 2^1A state (at 5.08 eV (244 nm) for *anti*-dG and 5.03 eV (247 nm) for *syn*-dG) of the $n \rightarrow \pi^*$ nature. As expected from its nature, the oscillator strength of 2^1A is weak (0.05 au) for *anti*-dG and very weak (0.01 au) for *syn*-dG. The states 4^1A, 5^1A, and 6^1A (at 5.91, 5.97, and 6.08 eV (210, 208, and 204 nm) for *anti*-dG and 5.90, 5.98, and 6.08 eV (210, 207, and 204 nm) for *syn*-dG) were calculated to be in the region of the third band at approximately 214 nm. The oscillator strength is almost zero for the $n \rightarrow \pi^*$ 4^1A and 6^1A states but is not zero for the $\pi \rightarrow \pi^*$ 5^1A state. However, these states were not observed in the experimental UV spectra because these three states are in the median of the two strong peaks (3^1A and 7^1A states), and their

dx.doi.org/10.1021/jp3085556 | J. Phys. Chem. A 2013, 117, 42−55

Table 1. SAC-CI UV and CD Spectra of *anti*- and *syn*-dG

	SAC-CI									
	anti-dG				*syn*-dG					
	EE[a]		osc[b]	rot[c]	EE[a]		osc[b]	rot[c]		
state	(eV)	(nm)	(au)	(10^{-40} cgs)	(eV)	(nm)	(au)	(10^{-40} cgs)	nature	exptl[d] (eV/nm)
1^1A	4.46	278	0.16	4.53	4.40	282	0.16	2.44	$\pi \rightarrow \pi^*$	4.49/276
2^1A	5.08	244	0.05	−76.31	5.03	247	0.01	38.12	$n \rightarrow \pi^*$	4.96/250
3^1A	5.10	243	0.20	68.20	5.06	245	0.22	−34.61	$\pi \rightarrow \pi^*$	4.96/250
4^1A	5.91	210	0.00	17.31	5.90	210	0.00	−2.92	$n \rightarrow \pi^*$	5.79/214
5^1A	5.97	208	0.02	−2.25	5.98	207	0.05	8.30	$\pi \rightarrow \pi^*$	5.79/214
6^1A	6.08	204	0.00	−2.15	6.08	204	0.00	−2.70	$n \rightarrow \pi^*$	5.79/214
7^1A	6.62	187	0.44	−7.82	6.54	189	0.38	−0.78	$\pi \rightarrow \pi^*$	

[a]Excitation energy. [b]Oscillator strength. [c]Rotatory strength. [d]Ref 35.

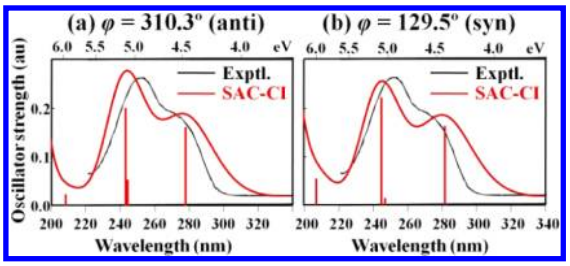

Figure 3. SAC-CI UV spectra of (a) *anti*- and (b) *syn*-dG (red), compared with the experimentally determined UV spectrum[35] of dG (black).

oscillator strengths are comparatively small. The 7^1A state (at 6.62 eV (187 nm) for *anti*-dG and 6.54 eV (189 nm) for *syn*-dG) was $\pi \rightarrow \pi^*$ (next-HOMO to LUMO and next-LUMO) excitation, which was assigned to the fourth band, compared with the experimental UV spectrum of deoxyguanosine monophosphate (dGMP).[55] Thus, the SAC-CI UV spectra of both *anti*- and *syn*-dG are similar to the experimental UV spectrum. The differences between the *anti*- and *syn*-dG were very small because the HOMO, next-HOMO, LUMO, and next-LUMO of the main configuration for 1^1A, 3^1A, and 7^1A states with large oscillator strengths are localized on the guanine site. Hence, we cannot determine if the experimental UV spectrum reflects that of either *anti*- or *syn*-dG.

3.2.2. CD Spectra of dG Monomer in Water. The SAC-CI CD spectra (red lines) of the dG monomer at several dihedral angles, φ were compared with the experimental CD spectrum (black line) above 200 nm (Figure 4). In the experimentally acquired spectra, the first band is at 276 nm, which is strong in the UV spectrum but very weak in the CD spectrum. The second band is at 250 nm, which is strong in both UV and CD spectra but has a negative sign in the CD spectrum. The third band at 214 nm is weak in the UV spectrum but strongly positive in the CD spectrum.

The SAC-CI CD spectra of dG with φ = 10−150 and 350° (Figure 4a−h,r) are quite different from the experimental CD spectrum. The SAC-CI CD spectrum of *syn*-dG (129.5°) is opposite in sign for the second band as compared with the experimental CD spectrum (Figure 4g). For dG with φ = 170, 210−290° (Figure 4i,k−o), the second band of the SAC-CI CD spectra agrees with the experimental CD spectrum, but the third band of the SAC-CI CD spectra has a weak intensity, compared with the experimental CD spectrum. The SAC-CI CD spectrum of the *anti*-dG and dG with φ = 330° (Figure 4p,q) is in good overall agreement with the experimental CD spectrum, with the second band being strongly negative and the third band being strongly positive.

As shown in Figure 2, the potential energy curve is flat around the anti conformer, and the energy barrier is not large. So, we calculated the ratio of the existence of each conformer, assuming the Boltzmann distribution at 275 K, a normal experimental condition, and using the ground state B3LYP/6-31G(d,p) energies. In Table 2, the column labeled "all" gives the ratio of each conformer when averaging included all 18 conformers, "anti" gives the ratio of each conformer when only seven conformations around anti are used, and "syn" gives the ratio of each conformer when only five conformations around syn are used. More than 70% of dG exists near the anti conformation between 270° and 330°, and about 11% exists near the *syn*-dG at 129.5°. Within the syn region (90−170°), more than 50% dG exist as the *syn*-dG (129.5°). However, in the anti region (250−10°), dG exists mostly between 270° and 330° as *anti*-dG. The gradient of the potential energy is sharp around the syn conformer but flat around the anti conformer because dG forms a hydrogen bond with the deoxyribose only in the syn conformation. Therefore, for the CD spectra, we may consider only the conformer at 129.5° for the syn conformer, but we have to consider several conformers around 310.3° for the anti conformer.

We also carried out the Boltzmann averaging for the spectra of the anti (Figure 4p) and syn (Figure 4g) conformations. The SAC-CI CD spectra of "all" (green), "anti" (blue), and single *anti*-dG (red) are similar to the experimental CD spectrum as shown in Figure 4p, while the SAC-CI CD spectra of "syn" (blue) and single *syn*-dG (red) are opposite in sign to the experimental CD spectrum (Figure 4g). These results confirm that *anti*-dG is the main conformation under the experimental condition. We note that the SAC-CI CD spectrum of dG at the single geometry of φ = 330° is more similar to the experimental CD spectrum of that of *anti*-dG (310.3°). This may indicate that dG with φ = 330° is more stable than the *anti*-dG in solution.

The dependence on the dihedral angle φ is very small in the UV spectrum of Figure 3 because only $\pi \rightarrow \pi^*$ has strong intensity. However, the CD spectra of Figure 4 strongly depend on the dihedral angle φ because both $\pi \rightarrow \pi^*$ and $n \rightarrow \pi^*$ have strong intensities, and their MOs, mainly localized at the guanine site, are somewhat extended to the deoxyribose. The 1^1A state assigned to the first band at 276 nm was calculated to have a small rotatory strength for both *anti*- and *syn*-dG, but this state was not observed in the experimental CD spectrum. In the second band region (250 nm), the rotatory strengths of

dx.doi.org/10.1021/jp3085556 | J. Phys. Chem. A 2013, 117, 42−55

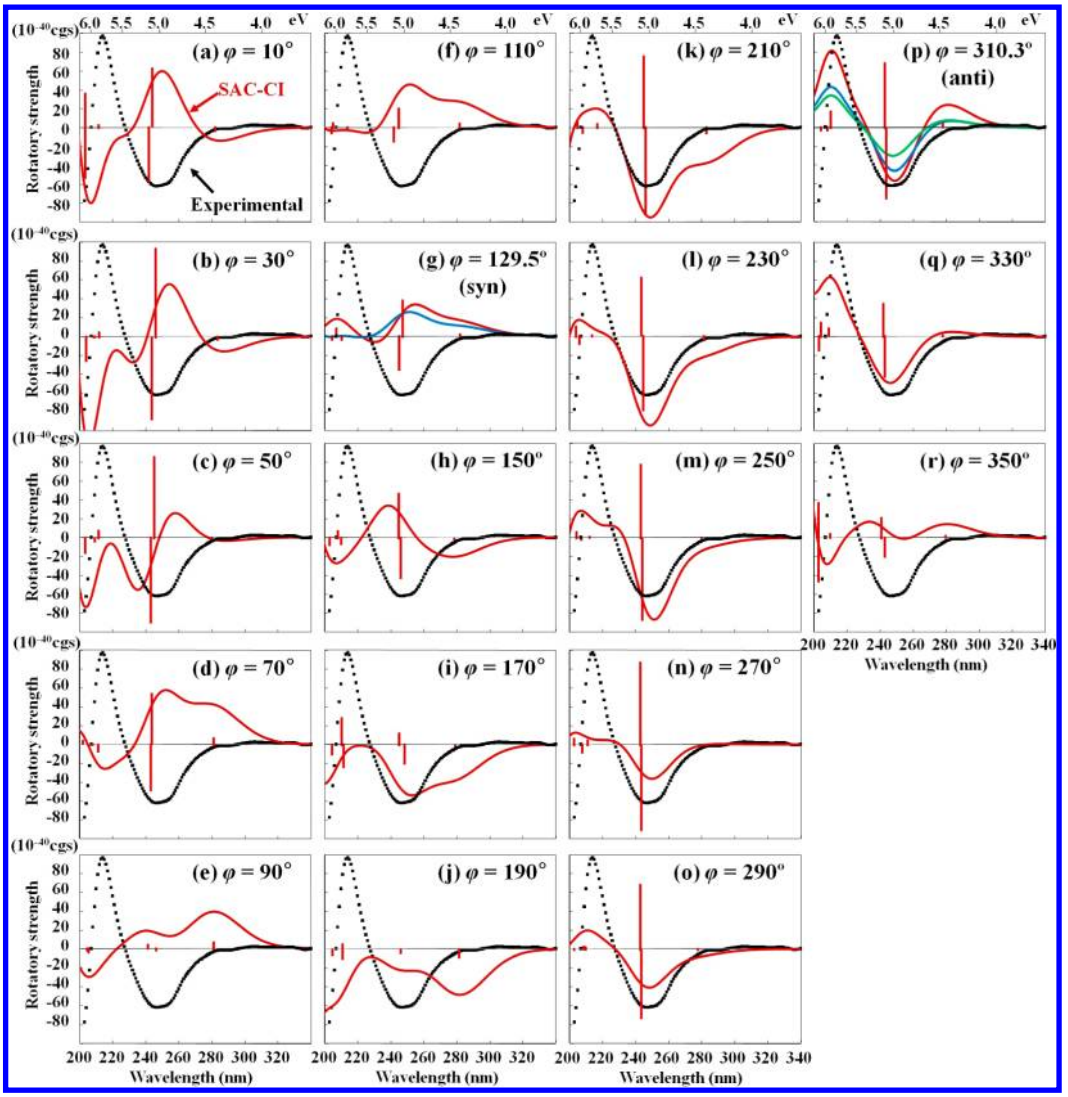

Figure 4. CD spectra of dG at several conformation angles φ. The experimental CD spectrum[35] (black line) of dG is compared with the SAC-CI CD spectra (red lines) of (a) $\varphi = 10°$, (b) $\varphi = 30°$, (c) $\varphi = 50°$, (d) $\varphi = 70°$, (e) $\varphi = 90°$, (f) $\varphi = 110°$, (g) $\varphi = 129.5°$ (syn), (h) $\varphi = 150°$, (i) $\varphi = 170°$, (j) $\varphi = 190°$, (k) $\varphi = 210°$, (l) $\varphi = 230°$, (m) $\varphi = 250°$, (n) $\varphi = 270°$, (o) $\varphi = 290°$, (p) $\varphi = 310.3°$ (anti), (q) $\varphi = 330°$, and (r) $\varphi = 350°$. The SAC-CI CD Boltzmann averaged spectra of (g) syn (blue line), (p) anti (blue line), and (p) all (green line) are also shown.

both the 2^1A and 3^1A states are large and opposite in sign (Table 1). The 2^1A state is calculated to lie at 5.08 eV (244 nm) for *anti*-dG and at 5.03 eV (247 nm) for *syn*-dG. The 3^1A state is calculated to lie at 5.10 eV (243 nm) for *anti*-dG and at 5.06 eV (245 nm) for *syn*-dG. The difference between 2^1A and 3^1A in the excitation energy is very small, so that their rotatory strengths cancel each other, giving relatively small rotatory strengths. From Table 1, we see that the total rotatory strength of the second band is negative for *anti*-dG and positive for *syn*-dG. To reproduce the experimental CD spectra, the theoretical rotatory strength must be reliable since, otherwise, reliable positive or negative CD peaks cannot be obtained. The SAC-CI theory seems to give reliable rotatory intensity since the theoretical CD spectra agree well with the experimental one. In the third band region (214 nm), the sum of the rotatory strengths is positive for both *anti*- and *syn*-dG, although the strongest rotatory strength comes from the 4^1A ($n \rightarrow \pi^*$) state for *anti*-dG but from the 5^1A ($\pi \rightarrow \pi^*$) state for *syn*-dG. As in the experimental CD spectrum, the third band has larger intensity than the second band in the SAC-CI CD spectrum of *anti*-dG. However, for *syn*-dG, the third band in the SAC-CI CD spectrum is smaller than the second band. The 7^1A state, assigned to the fourth band with a strong negative intensity at 190 nm in the experimental CD spectrum of dGMP,[55] is negative for *anti*-dG and almost zero for *syn*-dG.

3.3. Composite CD Spectra of dG and dC Compared with the CD Spectra of DNA. We then extended our studies to the spectra of B- and Z-DNA, and we compared the SAC-CI CD spectra of *anti*- and *syn*-dG (Figure 4) with the experimental CD spectra of B- and Z-DNA (Figure 5).[4] The second band at 250 nm in the SAC-CI CD spectrum of *anti*-dG is similar to the experimental CD spectrum of B-DNA, while the SAC-CI CD spectrum of *syn*-dG is similar to the experimental CD spectrum of Z-DNA. This result may indicate that, in DNA, the second band at 250 nm reflects the dihedral angle φ of dG between the deoxyribose and the guanine. Therefore, we calculated the composite SAC-CI CD spectra of the noninteracting dG and dC monomer from the available X-ray crystallographic structures in B- and Z-DNA to clarify if the different conformations of dG and/or dC in different types of DNA explain the differences in the CD spectra.

dx.doi.org/10.1021/jp3085556 | J. Phys. Chem. A 2013, 117, 42−55

Table 2. Boltzmann Distribution of dG along the Conformational Angle φ

angle (φ)	all (%)[a]	anti (%)[b]	syn (%)[c]
10	0.86	1.1	
30	0.14		
50	0.04		
70	0.10		
90	1.70		9.1
110	2.79		14.3
129.5 (syn)	11.31		51.7
150	4.54		22.4
170	0.41		2.5
190	0.08		
210	0.00		
230	0.10		
250	3.25	4.1	
270	15.34	19.5	
290	17.00	21.6	
310.3 (anti)	26.69	33.9	
330	13.07	16.6	
350	2.58	3.3	
total	100.0	100.0	100.0

[a]"all" gives the ratio of each conformer when averaging included all 18 conformers. [b]"anti" gives the ratio of each conformer when only seven conformations around anti are used. [c]"syn" gives the ratio of each conformer when only five conformations around syn are used.

The SAC-CI CD spectra of dG and dC alone (Figure 5a,b,d,e) having the structures of those in B- and Z-DNA and the composite CD spectra (Figure 5c,f) obtained as (a + b and d + e) were compared to the experimental CD spectra of B- and Z-DNA. The SAC-CI excitation energies, oscillator strengths, rotatory strengths, and natures of the excited states for the monomer model (dG and dC) were also determined (Table 3).

The conformations of dG and dC are the same as those in the ideal B-DNA or Z-DNA, in which dG and dC are arranged alternately (Figure 1). However, the X-ray structure was obtained for the DNA composed of only 6 sequences in the case of Z-DNA. Since the geometry is affected by the effect of the edge of DNA, the conformation is different for each monomer. Since the conformation of dG is, in particular, more flexible than that of dC in DNA, we calculated two kinds of dG (model I and II) in B- and Z-DNA, respectively. The models I and II correspond to dG of the hydrogen-bonding models (B-Hbond and Z-Hbond models) and the stacking models (B-Stack and Z-Stack models) of the dimer models, respectively. The dihedral angle (φ) between the deoxyribose and the guanine is 276.3° and 300.7°, respectively, for models I and II of B-DNA, and 111.3° and 117.5°, respectively, for models I and II of Z-DNA. The dihedral angle between the deoxyribose and cytosine is 323.2° for B-DNA and 332.9° for Z-DNA. The rotatory strength of dG is very different between models I and II for both B- and Z-DNA as shown in Table 3. Therefore, for dG, we prepared an averaged CD spectra for models I and II (Figure 5a,d). For Z-DNA, the SAC-CI CD spectrum of dG (Figure 5a) is negative for the first band and positive for the second band, as in the experimental spectrum of Z-DNA, although the excitation energies are calculated at a higher region. However, the SAC-CI result is opposite in sign to the experimental CD spectrum for the first band of B-DNA (Figure 5d). These results show that, in the CD spectra of DNA, the conformation of dG (monomer) is related to the sign of the second band but has no effect on the sign of the first band.

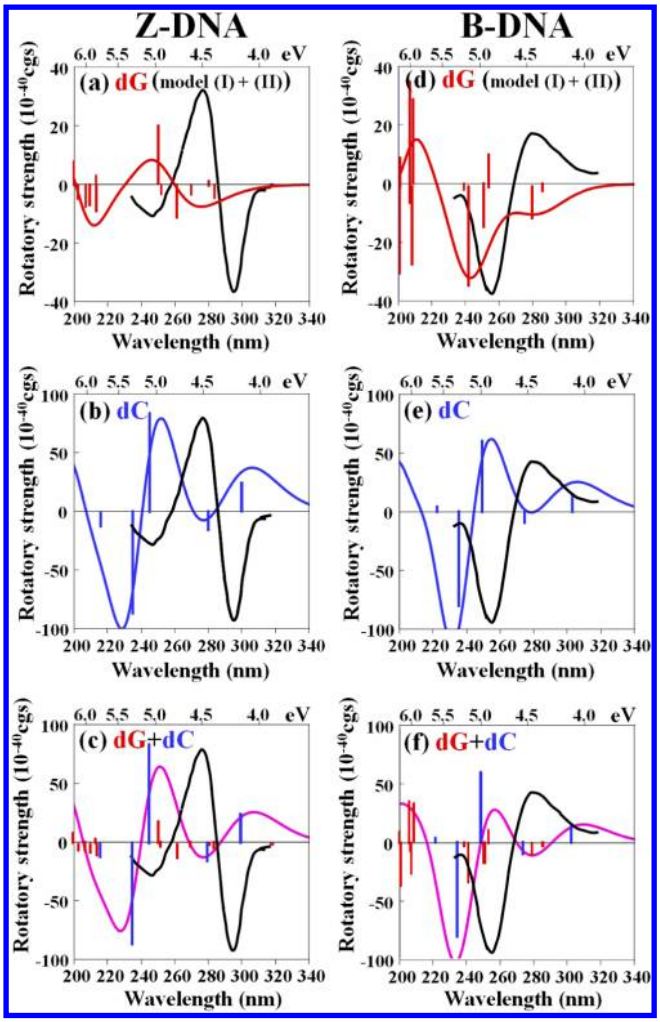

Figure 5. SAC-CI CD spectra of monomer ((a) dG in Z-DNA, (b) dC in Z-DNA, (d) dG in B-DNA, and (e) dC in B-DNA) and the composite CD spectra of (c) Z-DNA and (f) B-DNA obtained from the SAC-CI CD spectra of dG and dC, compared with the experimental CD spectra[4] (black lines) of Z-DNA (a–c) and B-DNA (d–f). The red and blue lines represent the excited state of dG and dC, respectively. The magenta line in panels c and f represents the composite spectra.

The CD spectra of dC have four peaks (Figure 5b,e). The first peak represents the $\pi-\pi^*$ of HOMO to LUMO. The second peak is the excitation from the nonbonding orbital to the LUMO. The third and fourth peaks are composed of both the $\pi-\pi^*$ and $n-\pi^*$ from next-HOMO and nonbonding orbitals to LUMO. The third and fourth peaks are mainly $\pi-\pi^*$ and $n-\pi^*$, respectively. The SAC-CI CD spectra of dC are similar in B- and Z-DNA, with two positive and two negative peaks. The rotatory strength is positive for the first and third peaks and negative for the second and fourth peaks. Therefore, the CD spectra of dC are always positive at around 295 nm, corresponding to the conformation of dC, which is always anti in DNA.

As shown in Figure 5c,f, the composite SAC-CI CD spectra obtained from dG and dC alone are similar between B- and Z-DNA. The sign at 295 nm is positive for both B- and Z-DNA because the rotatory strength of dC, which is the lowest peak, is much stronger than that of dG. Therefore, the composite CD

dx.doi.org/10.1021/jp3085556 | J. Phys. Chem. A 2013, 117, 42–55

Table 3. SAC-CI UV and CD Spectra of dG and dC in Z- and B-DNA

	Z-DNA					B-DNA				
	dG (model I, φ = 111.3°)					dG (model I, φ = 276.3°)				
	EE[a]		osc[b]	rot[c]		EE[a]		osc[b]	rot[c]	
state	(eV)	(nm)	(au)	(10^{-40} cgs)	nature	(eV)	(nm)	(au)	(10^{-40} cgs)	nature
1^1A	4.41	281	0.17	1.25	$\pi \rightarrow \pi^*$	4.43	280	0.16	−10.35	$\pi \rightarrow \pi^*$
2^1A	4.74	262	0.00	−10.99	$n \rightarrow \pi^*$	4.88	254	0.00	10.99	$n \rightarrow \pi^*$
3^1A	4.93	251	0.23	20.66	$\pi \rightarrow \pi^*$	5.13	242	0.25	−33.55	$\pi \rightarrow \pi^*$
4^1A	5.78	214	0.00	−8.64	$n \rightarrow \pi^*$	5.95	208	0.02	−26.19	$\pi \rightarrow \pi^*$
5^1A	5.91	210	0.04	−6.56	$\pi \rightarrow \sigma^*$	5.99	207	0.01	35.71	$n \rightarrow \pi^*$
6^1A	6.11	203	0.00	−4.38	$n \rightarrow \pi^*$	6.18	201	0.00	9.83	$n \rightarrow \pi^*$
7^1A	6.28	197	0.00	3.59	$\pi \rightarrow \sigma^*$	6.75	184	0.08	12.35	$\pi \rightarrow \sigma^*$
8^1A	6.59	188	0.30	6.34	$\pi \rightarrow \pi^*$	6.78	183	0.28	−24.02	$\pi \rightarrow \pi^*$
	dG (model II, φ = 117.5°)					dG (model II, φ = 300.7°)				
	EE[a]		osc[b]	rot[c]		EE[a]		osc[b]	rot[c]	
state	(eV)	(nm)	(au)	(10^{-40} cgs)	nature	(eV)	(nm)	(au)	(10^{-40} cgs)	nature
1^1A	4.37	284	0.16	−4.51	$\pi \rightarrow \pi^*$	4.34	286	0.16	−2.47	$\pi \rightarrow \pi^*$
2^1A	4.59	270	0.00	−3.22	$n \rightarrow \pi^*$	4.93	251	0.00	−14.67	$n \rightarrow \pi^*$
3^1A	4.91	252	0.22	−3.19	$\pi \rightarrow \pi^*$	5.18	239	0.21	−2.00	$\pi \rightarrow \pi^*$
4^1A	5.81	213	0.03	3.23	$\pi \rightarrow \pi^*$	5.95	209	0.01	28.84	$n \rightarrow \pi^*$
5^1A	5.98	207	0.00	−7.38	$\pi \rightarrow \pi^*$	5.99	207	0.03	−6.47	$\pi \rightarrow \pi^*$
6^1A	6.21	200	0.00	7.96	$n \rightarrow \pi^*$	6.17	201	0.00	−30.33	$n \rightarrow \pi^*$
7^1A	6.41	193	0.00	3.53	$\pi \rightarrow \sigma^*$	6.60	188	0.48	9.78	$\pi \rightarrow \pi^*$
8^1A	6.47	191	0.31	−0.77	$\pi \rightarrow \pi^*$	6.66	186	0.01	3.26	$\pi \rightarrow \sigma^*$
	dC (φ = 332.9°)					dC (φ = 323.2°)				
	EE[a]		osc[b]	rot[c]		EE[a]		osc[b]	rot[c]	
state	(eV)	(nm)	(au)	(10^{-40} cgs)	nature	(eV)	(nm)	(au)	(10^{-40} cgs)	nature
1^1A	4.13	300	0.09	23.85	$\pi \rightarrow \pi^*$	4.09	303	0.09	14.03	$\pi \rightarrow \pi^*$
2^1A	4.42	280	0.00	−15.48	$n \rightarrow \pi^*$	4.52	274	0.00	−9.15	$n \rightarrow \pi^*$
3^1A	5.07	245	0.11	83.92	$\pi + n \rightarrow \pi^*$	4.99	249	0.07	59.75	$\pi + n \rightarrow \pi^*$
4^1A	5.27	235	0.11	−86.39	$n + \pi \rightarrow \pi^*$	5.27	235	0.15	−80.17	$\pi + n \rightarrow \pi^*$
5^1A	5.73	216	0.00	−13.85	$n \rightarrow \pi^*$	5.59	222	0.01	3.93	$n \rightarrow \pi^*$
6^1A	6.32	196	0.39	23.49	$\pi \rightarrow \pi^*$	6.25	198	0.32	10.98	$\pi \rightarrow \pi^*$

[a]Excitation energy. [b]Oscillator strength. [c]Rotatory strength.

spectrum is similar to that of dC for both B- and Z-DNA. As a result, in the composite CD spectra of B- and Z-DNA, the sign at around 295 nm is independent of the geometry of the monomer (dG or dC), even though the CD spectrum of dG depends on the dihedral angle between the guanine and the deoxyribose, because the lowest peak originates from dC, whose geometry is always anti in both B- and Z-DNA. This indicates that the noninteracting dG and dC cannot explain the experimental spectra of DNA and that the hydrogen-bonding or stacking interactions with the neighboring nucleic acid bases must be important for the CD spectra of DNA.

3.4. UV and CD Spectra of Dimer Models. In the studies of the structure, spectroscopy, and functions of DNA, it is generally recognized that the hydrogen-bonding interaction and the stacking interaction are the two most important interactions that characterize the properties of DNA. So, we expect that these interactions might also be the important factors that affect the features of the UV and CD spectra of DNA. To investigate the possible origin, we considered the dimer model composed of dG and dC. These models contained either the hydrogen-bonding interaction or the stacking interaction (Figure 1). However, we note that the SAC-CI results using these models need not be in agreement with the experimental spectra because these models lack either the stacking interaction or the hydrogen-bonding interaction. We must use the tetramer model, at least, to compare with the experimental spectra as noted below.

3.4.1. UV Spectra of Dimer Models. Figure 6 shows the SAC-CI UV spectra of both hydrogen-bonding and stacking models of both B- and Z-DNA compared with the experimental UV spectrum. The experimental UV spectra of Z-DNA display a main peak at 256 nm and a shoulder peak at around 290 nm. The experimental UV spectrum of B-DNA is very similar, but the shoulder peak at around 290 nm is weaker. Table 4 shows the excitation energies, oscillator strengths, rotatory strengths, natures, and the types of the excited states of the SAC-CI results for both hydrogen-bonding and stacking models of the dimer. When the excitation in the dimer model is not within dG or dC, but corresponds to the electron transfer (ET) between dG and dC, we assigned it as the ET type.

The SAC-CI UV spectrum of the hydrogen-bonding model of Z-DNA (Z-Hbond model) is in good agreement with the experimental UV spectrum of Z-DNA (Figure 6a). Three strong peaks of the π−π^* nature are calculated. The lowest strong peak corresponds to the shoulder peak at 4.28 eV (290 nm) of the experimental UV spectrum of Z-DNA. The remaining two strong peaks correspond to the main peak at 4.84 eV (256 nm) of the experimental UV spectrum of Z-DNA. Red, blue, and green colors represent the excited states of dG, dC, and ET, respectively.

dx.doi.org/10.1021/jp3085556 | J. Phys. Chem. A 2013, 117, 42−55

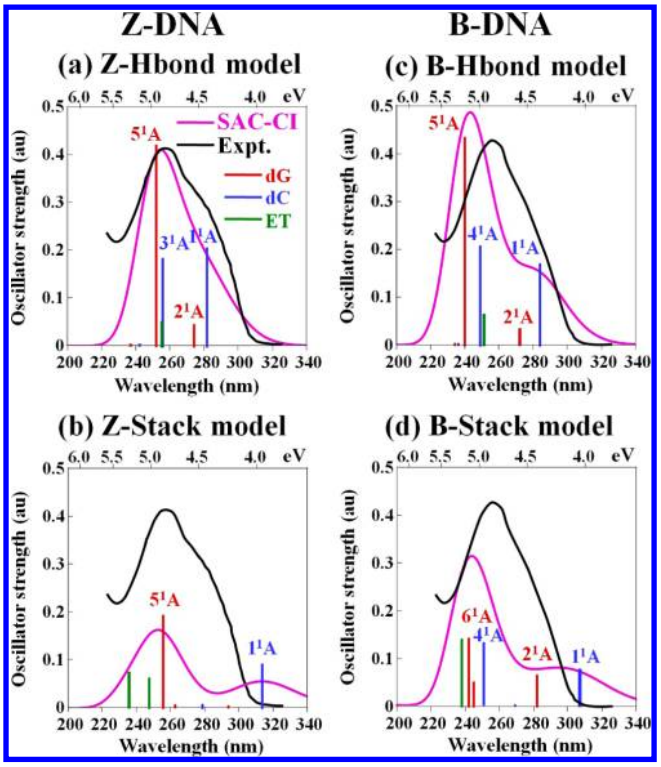

Figure 6. SAC-CI UV spectra for the dimer models. The SAC-CI spectra (magenta line) of (a) Z-Hbond model, (b) Z-Stack model, (c) B-Hbond model, and (d) B-Stack model are compared with the experimental UV spectra[4] (black line) of Z-DNA (a,b) and B-DNA (c,d). The red and blue lines represent the intramolecular excited states of dG and dC, respectively. The green lines represent the electron transfer (ET) excited state from dG to dC.

The shoulder peak in the experimental UV spectrum of Z-DNA is composed of 1^1A (4.39 eV) and 2^1A (4.53 eV) states. The 1^1A state (in blue color) of the Z-Hbond model corresponds to the 1^1A state of dC at 4.13 eV, which is the excitation from the HOMO to the LUMO of dC. This state has large oscillator strength of the $\pi-\pi^*$ nature. In the Z-Hbond model, this state is blue-shifted by 0.26 eV because the HOMO−LUMO gap (0.449 au) of the Z-Hbond model is larger than that (0.438 au) of dC. This state is in good agreement with the first (shoulder) peak of the experimental UV spectrum of Z-DNA. However, the 2^1A state (4.53 eV, red color) of the Z-Hbond model is assigned to the 3^1A state (4.93 eV) of dG, which is the excitation from the HOMO to the next-LUMO of dG. This large shift of the excitation energy is caused by the MO-order change. The MO of the Z-Hbond model, corresponding to the next-LUMO of dG, becomes lower than the MO of the Z-Hbond model, corresponding to the LUMO of dG, by the formation of hydrogen bonds with cytosine in the Z-Hbond model. Therefore, this state is red-shifted by 0.4 eV. However, the oscillator strength of this state is small, despite its $\pi-\pi^*$ nature. The transition moment is canceled because the main configuration includes not only the excitation from the HOMO to the next-LUMO in dG but also the excitation from the next-HOMO to the LUMO in dC and the electron transfer type excitation from the HOMO of dG to the LUMO and next-LUMO of dC.

The main peak of the experimental UV spectrum of Z-DNA is composed of 3^1A (4.84 eV) and 5^1A (4.93 eV) states having large oscillator strengths (Figure 6a). The 3^1A state (so blue color) of the Z-Hbond model is assigned to the 3^1A state (5.07 eV) of dC, which reflects the strong excitation from the next-HOMO to the LUMO of dC. The 5^1A state (red color) of the Z-Hbond model is assigned to the 1^1A state (4.41 eV) of dG, which is the excitation from the HOMO to the LUMO in dG. The excitation energy increases by 0.52 eV because the HOMO−LUMO gap becomes large, which is the opposite to that of the 2^1A state but again due to the hydrogen-bonding effect.

For B-DNA, however, the SAC-CI UV spectrum of the hydrogen-bonding model (B-Hbond model, Figure 6c) also has both main and shoulder peaks, in which the main peak is higher and the shoulder peak is lower, as compared with the experimental UV spectrum of B-DNA. The main peak (4^1A and 5^1A states) of the SAC-CI spectra of the B-Hbond model is higher than that of the experimental spectra similarly to the SAC-CI spectrum of the Z-Hbond model. The 3^1A state of dG in B-DNA is also higher than that in Z-DNA (Table 3). These results may be related to the fact that dG is more flexible than dC because the conformation of dG is anti for B-DNA but syn for Z-DNA. Since the stacking interaction of B-DNA is weaker than that of Z-DNA, the X-ray structure of B-DNA may be more flexible than that of Z-DNA. However, the result that the oscillator strength of the lowest excited state of the B-Hbond model is weaker than that of the Z-Hbond model is reflected by the fact that the shoulder peak of the experimental UV spectra is stronger in Z-DNA but weaker in B-DNA.

For the SAC-CI UV spectra of the stacking models of both B- (B-Stack model) and Z-DNA (Z-Stack model), the first excited states originated from dC were calculated at the lower-energy region (higher wavelength region), but the excitation energy of the main peak is almost the same between the B-Hbond and B-Stack models or between the Z-Hbond and Z-Stack models. If there is no hydrogen-bonding interaction in DNA, the lowest excited state would be observed in the lower-energy region of the experimental spectra, separately from the main peak. The excitation energy of the lowest excited state of the stacking model is lower than that of the hydrogen-bonding model by 0.44 eV for Z-DNA and 0.33 eV for B-DNA, respectively. This result may correspond to the fact that the lowest excitation energy of cytosine differs between the gas phase (4.28 eV)[56] and in solution (4.64 eV).[57]

For both B- and Z-DNA, the SAC-CI results of the hydrogen-bonding models (B-Hbond and Z-Hbond) are in better agreement with the experimental spectra than those of the stacking models (B-Stack and Z-Stack). Thus, the hydrogen-bonding interaction is reflected in the UV spectra of DNA. On the other hand, the shoulder peak observed for Z-DNA may reflect the stronger shoulder nature of the Z-Stack model in Z-DNA. However, the UV spectra of DNA provide little information about stacking interactions between nucleic acid bases.

3.4.2. CD Spectra of Dimer Models. Figure 7 shows the SAC-CI CD spectra of both hydrogen-bonding and stacking models of B- and Z-DNA compared with the experimental CD spectra. In the experimental CD spectra, the first peak is negative at 296 nm and the second peak is positive at 275 nm for Z-DNA. However, B-DNA displays peaks that are opposite in sign: the first peak is positive at 280 nm and the second peak is negative at 255 nm.

It is worth nothing that the SAC-CI spectrum has a negative peak at 295 nm only for the stacking model of Z-DNA (Z-Stack), but for the other models, the SAC-CI spectrum is

dx.doi.org/10.1021/jp3085556 | J. Phys. Chem. A 2013, 117, 42−55

Table 4. SAC-CI UV and CD Spectra of the Hydrogen-Bonding and Stacking Dimer Models of Z- and B-DNA

	Z-DNA							B-DNA						
	SAC-CI of Z-Hbond						exptl[e]	SAC-CI of B-Hbond						exptl[e]
	EE[a]		osc[b]	rot[c]			UV	EE[a]		osc[b]	rot[c]			UV
state	(eV)	(nm)	(au)	(10^{-40} cgs)	nature	type[d]	(eV/nm)	(eV)	(nm)	(au)	(10^{-40} cgs)	nature	Type[d]	(eV/nm)
1^1A	4.39	282	0.20	35.13	$\pi \rightarrow \pi^*$	dC (1^1A)	4.28/290	4.37	284	0.17	11.43	$\pi \rightarrow \pi^*$	dC (1^1A)	
2^1A	4.53	274	0.04	8.84	$\pi \rightarrow \pi^*$	dG (3^1A)		4.56	272	0.03	−14.81	$\pi \rightarrow \pi^*$	dG (3^1A)	
3^1A	4.84	256	0.18	9.12	$\pi \rightarrow \pi^*$	dC (3^1A)		4.93	251	0.06	5.83	$\pi \rightarrow \pi^*$	ET	
4^1A	4.85	255	0.05	−11.45	$\pi \rightarrow \pi^*$	ET		4.98	249	0.21	17.67	$\pi \rightarrow \pi^*$	dC (3 + 4^1A)	
5^1A	4.93	252	0.42	11.82	$\pi \rightarrow \pi^*$	dG (1^1A)	4.84/256	5.18	240	0.43	−13.90	$\pi \rightarrow \pi^*$	dG (1^1A)	4.84/256
6^1A	5.12	242	0.00	0.57	$n \rightarrow \pi^*$	dC (2^1A)		5.25	236	0.00	−11.97	$n \rightarrow \pi^*$	dC (2^1A)	
7^1A	5.23	237	0.00	−13.84	$n \rightarrow \pi^*$	dG (2^1A)		5.29	234	0.00	−5.79	$n \rightarrow \pi^*$	dG (2 + 5^1A)	
8^1A								6.23	199	0.00	−0.34	$n \rightarrow \pi^*$	dG (2 + 5^1A)	
	SAC−CI of Z-Stack						exptl[e]	SAC−CI of B-Stack						exptl[e]
	EE[a]		osc[b]	rot[c]			CD	EE[a]		osc[b]	rot[c]			CD
state	(eV)	(nm)	(au)	(10^{-40} cgs)	nature	type[d]	(eV/nm)	(eV)	(nm)	(au)	(10^{-40} cgs)	nature	type[d]	(eV/nm)
1^1A	3.95	314	0.09	−45.11	$\pi \rightarrow \pi^*$	dC (1^1A)	4.19/296	4.04	307	0.07	43.58	$\pi \rightarrow \pi^*$	dC (1^1A)	4.43/280
2^1A	4.21	294	0.00	−33.49	$\pi \rightarrow \pi^*$	dG (1^1A)	4.19/296	4.40	282	0.06	−10.32	$\pi \rightarrow \pi^*$	dG (1^1A)	
3^1A	4.45	279	0.01	29.67	$n \rightarrow \pi^*$	dC (2^1A)		4.61	269	0.00	−5.03	$n \rightarrow \pi^*$	dC (2^1A)	
4^1A	4.72	263	0.00	−13.35	$n \rightarrow \pi^*$	dG (2^1A)		4.93	251	0.13	94.07	$\pi \rightarrow \pi^*$	dC(3 + 4^1A)	
5^1A	4.85	256	0.19	−17.96	$\pi \rightarrow \pi^*$	dG (3^1A)	4.51/275	5.07	245	0.05	−151.15	$n \rightarrow \pi^*$	dG (2^1A)	4.86/255
6^1A	4.99	248	0.06	48.61	$\pi \rightarrow \pi^*$	ET	4.51/275	5.12	242	0.14	−110.56	$\pi \rightarrow \pi^*$	dG (3^1A)	4.86/255
7^1A	5.26	236	0.07	27.21	$\pi \rightarrow \pi^*$	ET + dC (3^1A)	4.51/275	5.21	238	0.14	194.75	$\pi \rightarrow \pi^*$	ET + dG(3^1A)	
8^1A	5.65	219	0.00	−2.31	$n \rightarrow \pi^*$	dC (4^1A)		6.19	200	0.00	−8.05	$n \rightarrow \pi^*$	dG (4^1A)	

[a]Excitation energy. [b]Oscillator strength. [c]Rotatory strength. [d]dG represents intramolecular excited states of dG, dC represents intramolecular excited states of dC, and ET represents electron transfer excited states from dG to dC. [e]Ref 4.

dx.doi.org/10.1021/jp3085556 | J. Phys. Chem. A 2013, 117, 42−55

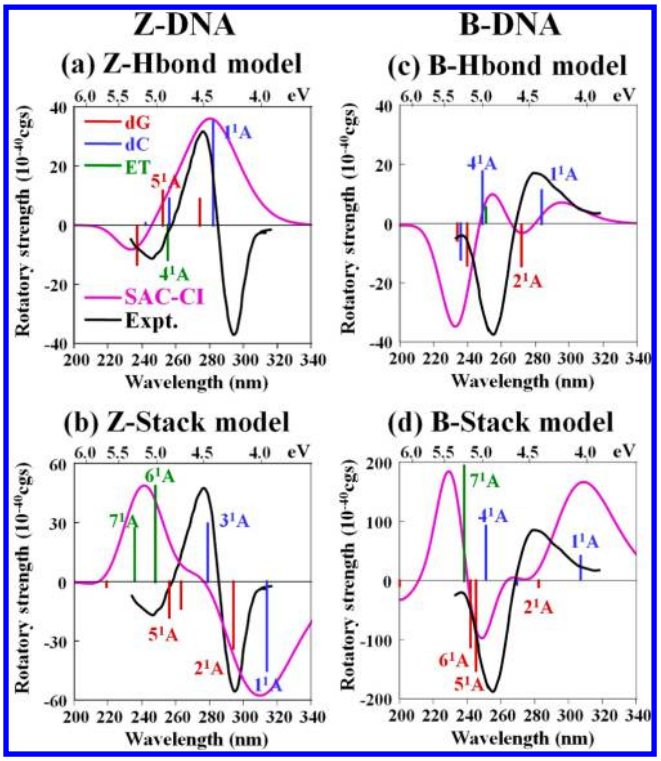

Figure 7. SAC-CI CD spectra for the dimer models. The SAC-CI spectra (magenta line) of (a) Z-Hbond model, (b) Z-Stack model, (c) B-Hbond model, and (d) B-Stack model are compared with the experimental CD spectra[4] (black line) of Z-DNA (a,b) and B-DNA (c,d). The red and blue lines represent the intramolecular excited states of dG and dC, respectively. The green lines represent the electron transfer (ET) excited state from dG to dC.

positive at 295 nm. Therefore, the strong negative sign of the CD spectra at 295 nm indicates that a strong stacking interaction exists in Z-DNA. The SAC-CI CD spectra of both stacking models (B-Stack and Z-Stack models) more closely resemble the experimental CD spectra of B- and Z-DNA than those of the hydrogen-bonding models (B-Hbond and Z-Hbond models). For the SAC-CI CD spectrum of the Z-Stack model, the first and second peaks are negative and positive, respectively, but they are the opposite of those obtained from the Z-Hbond model. For the B-Stack and B-Hbond models, however, the first peak is positive in the SAC-CI CD spectra, but the second and third peaks are negative and positive, respectively, for the B-Stack model in opposition to the B-Hbond model. Since the stacking models do not have the hydrogen-bonding interactions, the excitation energy of the first peak is lower than that of the experimental spectrum, as noted above.

In the Z-Stack model, the first peak with a negative sign is assigned to the 1^1A (3.95 eV) and 2^1A (4.21 eV) states (Table 4). The 1^1A state of the Z-Stack model corresponds to the 1^1A state (4.13 eV) of dC, which is the excitation of the $\pi-\pi^*$ from the HOMO to the LUMO in dC. A large oscillator strength is the origin of the first (shoulder) peak but the excitation energy is lower than the experimental value because there is no hydrogen bond in the Z-Stack model. The rotatory strength of the 1^1A state of dC changes the sign from positive to negative by the stacking interaction with dG. Therefore, the stacking interaction between dG and dC accounts for the strong negative sign of the CD spectra in Z-DNA.

The excitation energy of the 2^1A state (4.21 eV) is also close to the first peak of the experimental CD spectrum. This state is assigned to the 1^1A state (4.37 eV) of dG, which is the HOMO to LUMO $\pi-\pi^*$ excitation in dG but also includes the contribution of the excitation from the next-HOMO to LUMO in dC. The oscillator strength in the UV spectrum is small because this state differs from the 1^1A state of dG by the inclusion of the excitation in dC. Although the excitation energy is shifted by the formation of hydrogen bonds between dG and dC, the rotatory strength of a large negative may contribute to the strong negative sign of the CD spectra in Z-DNA. In the 3^1A state (4.45 eV), which is the excitation from nonbonding orbital to the LUMO in dC, the rotatory strength changes to positive from the negative sign of the monomer dC. However, this state is not the origin of the second peak as will be noted later in the tetramer model section. Thus, the rotatory strength is strongly affected by the stacking interaction.

Three important excited states are calculated in the higher-energy region of the second peak. The 5^1A state (4.85 eV) has the largest oscillator strength and is assigned to the 3^1A (4.91 eV) state of dG, which is the excitation from HOMO to next-LUMO. This state is assigned to the main peak (4.84 eV) of the experimental UV spectrum of Z-DNA. The 6 and 7^1A states (4.99 and 5.26 eV) with a large rotatory strength are the ET state from the HOMO of dG to the LUMO of dC. The main configuration of the 7^1A state also includes the excitation from the next-HOMO to the LUMO in dC.

In the B-Stack model, the first peak with a positive sign is assigned to the 1^1A state (4.04 eV). This state corresponds to the 1^1A state (4.09 eV) of dC, which is the excitation from the HOMO to the LUMO. The 2^1A state (4.40 eV) is assigned to the 1^1A state (4.34 eV) of dG, which reflects the excitation from the HOMO to the LUMO. Since the B-Stack model does not have hydrogen bonds, the excitation energies are close to those of dG or dC. Both states have the oscillator strength but the 1^1A state is positive, while the 2^1A state is slightly negative for the rotatory strength, which is the same as for the monomers dC and dG, respectively. Therefore, the stacking interaction of B-DNA has little effect on the sign of the CD spectra at 295 nm because the stacking interaction is weaker in B-DNA than in Z-DNA.

The second peak with a negative sign is assigned to the 5 and 6^1A states with a large rotatory strength. The 5 and 6^1A states (5.07 and 5.12 eV in Table 4) are assigned to the 2 and 3^1A states (4.93 and 5.18 eV in Table 3) of dG, which are the excitations from the nonbonding orbital and the HOMO to the next-LUMO. The main configuration is $n-\pi^*$ for the 5^1A state and $\pi-\pi^*$ for the 6^1A state. Both states have strong oscillator and negative rotatory strengths, which means that they can be assigned to the main peaks.

The first ET excited states (7^1A state, 5.21 eV) of B-Stack model are calculated at a higher region than that (6^1A state, 4.99 eV) of the Z-Stack model because the stacking interaction is weaker in B-DNA than in Z-DNA.

The SAC-CI results show that both hydrogen-bonding and stacking interactions affect the UV and CD spectra of DNA. In particular, the excitation energy of the first excited state increases by the formation of hydrogen bonds and the stacking interaction changes the sign of the CD spectrum of the first excited state from positive to negative. The strong stacking interaction characteristic of the helical structure of Z-DNA is the origin of the strong negative sign at around 295 nm in the CD spectra. The hydrogen-bonding and stacking interactions

dx.doi.org/10.1021/jp3085556 | J. Phys. Chem. A 2013, 117, 42−55

also confer other smaller effects on the UV and CD spectra of DNA. In the higher energy region, the SAC-CI CD spectra are not in good agreement with the experimental CD spectra because these models have either hydrogen-bonding interaction or stacking interaction, but not both. Therefore, we need to investigate a better model that includes both hydrogen bonding and stacking interactions, within the same model. A minimum such model is the tetramer model of Figure 1, on which we explain in the next section.

3.5. Tetramer Model. The SAC-CI calculations of the dimer models were suitable to investigate the effects of the hydrogen-bonding interaction and the stacking interaction, separately. For example, the SAC-CI UV spectra of the hydrogen-bonding models were in good agreement with the experimental UV spectra, implying the importance of the hydrogen-bonding interaction. The SAC-CI CD spectra for the stacking model clarified that the stacking interaction is the source of the negative CD peak at around 295 nm. However, generally speaking, the SAC-CI CD spectra were markedly different from the experimental spectra. The SAC-CI UV spectra of the stacking models were composed of two peaks, different from the experimental UV spectra. Thus, the information that we gained from the dimer models still did not fully resolve these differences in the spectra acquired by two different processes. So we used the tetramer model (Figure 1), which included both hydrogen-bonding and stacking interactions within the same model.

Figure 8 shows the SAC-CI UV and CD spectra of the tetramer model of Z-DNA (Z-Tetra model) and B-DNA (B-Tetra model), in comparison with the experimental UV and CD spectra. In order to compare the experimental spectra, the SAC-CI results were shifted to lower energy by 0.5 eV. The computational conditions were poor, as compared with the other SAC-CI calculations. In the tetramer calculations, the d-polarization functions were not added, and the small active space was used. The SAC-CI calculations using the small active space and without the d-polarization functions gave higher excitation energies by about 0.4−0.5 eV (see Supporting Information, Table S1) for the hydrogen-bonding dimer models. In particular, the excited states corresponding to the main peak of the experimental UV spectra were shifted by 0.48 eV for both the Z-Hbond model (6^1A state) and the B-Hbond model (7^1A state).

Table 5 shows the excitation energies, oscillator strengths, rotatory strengths, natures, and type of the excited states of the SAC-CI results for tetramer models.

The SAC-CI UV spectrum of the Z-Tetra model is in good agreement with the experimental UV spectrum of Z-DNA. The main peak as well as the shoulder peak is reproduced by the SAC-CI method. The shoulder peak is assigned to the 4 and 5^1A states, which is the $\pi-\pi^*$ excitation (HOMO to LUMO) in dC, and the main peak is assigned to the 10^1A state, which is the $\pi-\pi^*$ (HOMO to next-LUMO) excitation in dG.

The SAC-CI UV spectrum of the B-Tetra model is also in a reasonable agreement with the experimental UV spectrum of B-DNA, although the shape of the shoulder is slightly different. In the B-Tetra model, the shoulder peak is assigned to the 2^1A state, which is the $\pi-\pi^*$ (HOMO to LUMO) excitation in dC, and the main peak is assigned to the 8^1A state, which is the $\pi-\pi^*$ (HOMO to next-LUMO) excitation in dG.

The sign of the rotatory strength is the same between the SAC-CI CD spectrum of the Z-Tetra model and the experimental CD spectrum of Z-DNA, although the negative

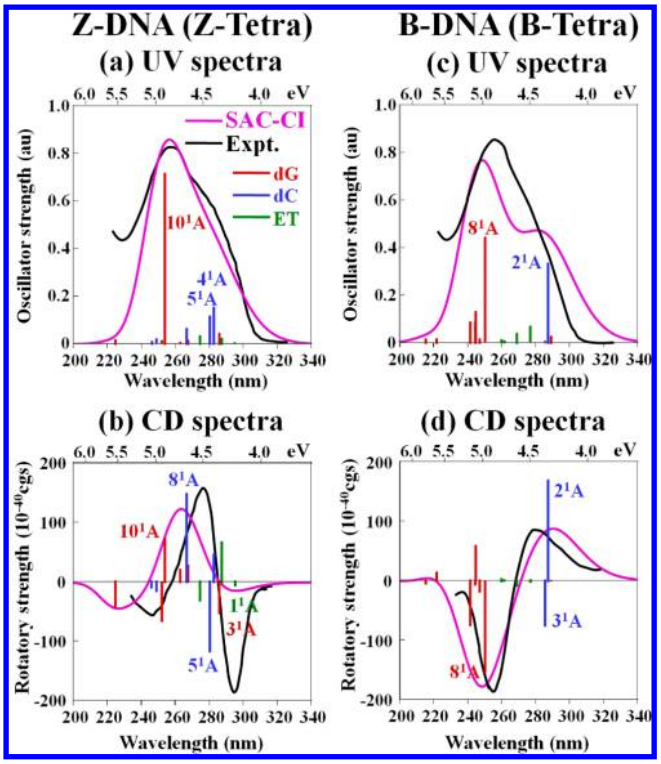

Figure 8. SAC-CI UV and CD spectra for the tetramer models. The SAC-CI spectra (magenta line) of Z-Tetra model (a,b) and B-Tetra model (c,d) as compared with the experimental UV and CD spectra[4] (black line) of Z-DNA (a,b) and B-DNA (c,d). The red and blue lines represent the intramolecular excited states of dG and dC, respectively. The green lines represent the electron transfer (ET) excited state from dG to dC. All excited states of SAC-CI calculations have been shifted to the lower values by 0.5 eV.

rotatory strength at 295 nm is very weak because the polarization functions were not included in the tetramer models. It is well-known that the basis set must be good for an adequate description of the stacking interaction.[58,59] In the dimer model, the lack of polarization d-functions and the smaller active space changed the intensity and sign of the rotatory strength (see Supporting Information, Table S1).

Since the stacking interaction is small in B-DNA, the SAC-CI CD spectrum of the B-Tetra model is in good agreement with the experimental CD spectrum of B-DNA and reproduces not only the sign of the rotatory strength but also the overall shape of the spectrum.

In Z-DNA, the 1^1A state is assigned to the first peak of the experimental CD spectrum. The 1^1A state is the ET excitation from the HOMO of dG to the LUMO of dC through the stacking conformation. The 3 and 5^1A states with a large negative rotatory strength are the excitation from the HOMO to the LUMO in dG and dC, respectively. These states also contribute to the first negative peak, as in the 1 and 2^1A states with a negative rotatory strength in the Z-Stack model. The 8 and 10^1A states are assigned to the second peak of the CD spectrum. The 10^1A state, which is the origin of the main peak of the UV spectrum, and the $\pi-\pi^*$ of dC (8^1A state) also contribute to the second peak of the CD spectrum.

In B-DNA, the first peak of the CD spectrum is assigned to the 2^1A state of $\pi-\pi^*$ (HOMO to LUMO) in dC, which is the same as the origin of the first peak of the UV spectrum. The ET states are calculated at the higher energy region than the 2^1A

dx.doi.org/10.1021/jp3085556 | J. Phys. Chem. A 2013, 117, 42−55

Table 5. SAC-CI UV and CD Spectra of the Tetramer Models of Z- and B-DNA

	Z-DNA								B-DNA							
	SAC−CI of Z-Tetra							exptl[e]	SAC-CI of B-Tetra							exptl[e]
	EE[a]		Osc[b]	Rot[c]			UV	CD	EE[a]		Osc[b]	Rot[c]			UV	CD
state	(eV)	(nm)	(au)	(10^{-40} cgs)	nature	type[d]	(eV/nm)	(eV/nm)	(eV)	(nm)	(au)	(10^{-40} cgs)	nature	type[d]	(eV/nm)	(eV/nm)
1^1A	4.70	264	0.00	−6.63	$\pi \rightarrow \pi^*$	ET		4.19/296	4.79	259	0.03	−0.41	$\pi \rightarrow \pi^*$	dG		
2^1A	4.81	258	0.02	66.11	$\pi \rightarrow \pi^*$	ET			4.82	257	0.33	168.91	$\pi \rightarrow \pi^*$	dC		4.43/280
3^1A	4.84	256	0.04	−53.26	$\pi \rightarrow \pi^*$	dG		4.19/296	4.84	256	0.01	−74.54	$\pi \rightarrow \pi^*$	dC		
4^1A	4.88	254	0.15	45.53	$\pi \rightarrow \pi^*$	dC	4.28/290		4.98	249	0.07	−1.30	$\pi \rightarrow \pi^*$	ET		
5^1A	4.92	252	0.12	−117.12	$\pi \rightarrow \pi^*$	dC	4.28/290	4.19/296	5.11	243	0.04	−6.22	$\pi \rightarrow \pi^*$	ET		
6^1A	5.02	247	0.03	−30.34	$\pi \rightarrow \pi^*$	ET			5.25	236	0.00	−0.46	$\pi \rightarrow \pi^*$	ET		
7^1A	5.13	242	0.01	27.37	$n \rightarrow \pi^*$	dG			5.27	235	0.01	3.32	$\pi \rightarrow \pi^*$	ET		
8^1A	5.15	241	0.06	147.72	$\pi \rightarrow \pi^*$	dC		4.51/275	5.45	227	0.45	−156.09	$\pi \rightarrow \pi^*$	dG	4.84/256	4.86/255
9^1A	5.22	238	0.01	19.78	$n \rightarrow \pi^*$	dG			5.52	225	0.02	−17.95	$n \rightarrow \pi^*$	dG		
10^1A	5.38	230	0.71	72.99	$\pi \rightarrow \pi^*$	dG	4.84/256	4.51/275	5.56	223	0.13	59.29	$\pi \rightarrow \pi^*$	dG		
11^1A	5.41	229	0.01	−68.58	$\pi \rightarrow \pi^*$	dG			5.58	222	0.09	−5.25	$\pi \rightarrow \pi^*$	dG		
12^1A	5.48	226	0.02	−15.19	$n \rightarrow \pi^*$	dC			5.63	220	0.08	−74.36	$n \rightarrow \pi^*$	dG		
13^1A	5.53	224	0.01	−9.24	$n \rightarrow \pi^*$	dC			6.09	204	0.01	13.79	$n \rightarrow \pi^*$	dG		
14^1A	6.01	206	0.01	−41.59	$n \rightarrow \pi^*$	dG			6.26	198	0.02	−4.64	$n \rightarrow \pi^*$	dG		

[a]Excitation energy. All excited states of SAC-CI calculations have been shifted to the lower values by 0.5 eV in Figure 8. [b]Oscillator strength. [c]Rotatory strength. [d]dG represents intramolecular excited states of dG, dC represents intramolecular excited states of dC, and ET represents electron transfer excited states from dG to dC. [e]Ref 4.

dx.doi.org/10.1021/jp3085556 | J. Phys. Chem. A 2013, 117, 42−55

state because the stacking interaction is weaker in B-DNA than in Z-DNA (Figure 1). Therefore, the first peak of the experimental CD spectra originates from the ET excitation from dG to dC for Z-DNA but corresponds to the intramolecular excitation in dC for B-DNA. The second peak with a negative sign is assigned to the 8^1A state. The 8^1A state, which is the $\pi-\pi^*$ of dG, is the origin of both the main peaks of the UV spectrum and the second peak of the CD spectrum.

The ET excited states of the tetramer models were calculated at a lower energy region than those of the dimer models for both B- and Z-DNA. This result may be related to the overlap between the nucleic acid bases. The overlap exists only in part of the nucleic acid bases in the dimer models, but in the tetramer models, the overlap covers the hydrogen bonds as well as the nucleic acid bases. The ET excited states are important for the CD spectrum of Z-DNA because the lowest excited state is the ET type and is negative for rotatory strength, but for B-DNA, the ET excited states are not important because these states are weak in both oscillator and rotatory strengths.

The SAC-CI results of the tetramer models are calculated at a higher region by about 0.5 eV because of the small active space. Therefore, better SAC-CI calculations are required for comparison with the experimental UV and CD spectra of DNA. However, these results indicate that the strong stacking interaction characteristic of the helical structure of Z-DNA changes the sign of the rotatory strength for the lowest excited states of dG and dC and produces the emergence of the ET excited states.

4. CONCLUSIONS

DNA chemistry is affected by three important factors: (1) the conformation of the monomer (dG), which is related to the dihedral angle between deoxyribose and guanine; (2) the hydrogen-bonding interactions; and (3) the stacking interactions between two nucleic acid bases. To verify whether these three factors are important for the CD spectra of DNA, we examined four different models using the SAC-CI method.

(1) dG monomer model: We first applied the SAC-CI method to the dG monomer to examine the effect of conformation on the CD spectra of dG and, from this result, to identify the structure of the dG monomer in solution. Our calculations showed that the shape and the sign of the CD spectra depend strongly on the dihedral angle between the deoxyribose and the guanine, but that the SAC-CI UV spectra of both *anti*- and *syn*-dG are very similar because the UV spectra are not strongly dependent on the conformation. The experimental CD spectrum agreed with the theoretical spectrum of dG only for the anti conformation. The resulting thermally averaged spectra also support the anti geometry of dG as a stable conformation in solution. However, the SAC-CI CD spectrum of *syn*-dG is opposite in sign from that of the experimental spectrum. Thus, the SAC-CI CD spectra of dG in both anti and syn conformations do not explain the negative sign at 295 nm of the CD spectra of the DNA composed of dG and dC.

(2) Composit model of dG and dC monomers: A comparison of the calculated composite spectra of dG and dC with the experimental spectra of the two-component DNA showed similarities between B- and Z-DNA because the conformation of dC is always anti in both B- and Z-DNA. The SAC-CI results led us to confirm that that the conformation of dG is *not* the origin of the negative peak at 295 nm in Z-DNA.

(3) Dimer model: Our examination of the dimer model permitted us to investigate the separate importance of the hydrogen-bonding and the stacking interactions in the structural chemistry of B- and Z-DNA. The SAC-CI calculations showed that the hydrogen-bonding interactions change the excitation energies and that the stacking interactions are responsible for the changes in the sign of the CD rotatory strength. The SAC-CI UV spectra of the hydrogen-bonding models (B-Hbond and Z-Hbond models) are similar to the experimental UV spectra in which the main peak as well as the shoulder peak is well reproduced. The SAC-CI CD spectra of the stacking models (B-Stack and Z-Stack models) have the same sign as the experimental CD spectra. We concluded that the stacking interaction is especially important for the CD spectrum of the strongly stacked Z-DNA because the CD signal at 295 nm changed to a negative sign only for the Z-Stack model.

(4) Tetramer model: Finally, our calculations with the tetramer model that contain both hydrogen-bonding and stacking interactions revealed that the shape of the SAC-CI UV and CD spectra compared well with the experimental ones. The ET excitations as well as the lowest intramolecular excitation of dC and dG are the origins of the negative sign of the experimental CD spectrum of Z-DNA. The ET excited state is calculated at a lower energy region than the intramolecular excited states of dG or dC for the strongly stacked Z-DNA but at a higher energy region for the weakly stacked B-DNA. The negative sign of the first peak of the experimental CD spectra of Z-DNA is due to the strong stacking effect characteristic of its helical structure.

The dynamic behavior of the dG monomer in solution was partially considered by taking the Boltzmann averaging of the calculated spectra over the various conformations. Fortunately, the Boltzmann averaged SAC-CI CD spectrum was in good agreement with the experimental spectra, although the SAC-CI CD spectra largely depend on the conformation of dG. However, in this study, we used only the static model for dimer and tetramer models. The SAC-CI CD results of the dimer and tetramer models explained the difference between the experimental CD spectra of B- and Z-DNA. However, since the structure of DNA would also be flexible in solution, it is necessary to take into account the dynamic behavior of DNA. This is an important and interesting topic.

■ ASSOCIATED CONTENT

Ⓢ Supporting Information

SAC-CI results of the hydrogen-bonding and stacking dimer models of Z- and B-DNA using small active space and without the polarization d-functions. This material is available free of charge via the Internet at http://pubs.acs.org.

■ AUTHOR INFORMATION

Corresponding Author

*Phone: +81-75-634-3211. Fax: +81-75-634-3211. E-mail: h.nakatsuji@qcri.or.jp.

Notes

The authors declare no competing financial interest.

■ ACKNOWLEDGMENTS

The computations were performed at the Research Center for Computational Science, Okazaki, Japan.

REFERENCES

(1) Voet, D., Voet, J. G., Eds. *Biochemistry*; John Wiley & Sons, Inc.: New York, 1995.
(2) Ghosh, A.; Bansal, M. *Acta Crystallogr.* **2003**, *D59*, 620−626.
(3) Rich, A.; Nordheim, A.; Wang, A. H.-J. *Annu. Rev. Biochem.* **1984**, *53*, 791−846.
(4) Tran-Dinh, S.; Taboury, J.; Neumann, J.-M.; Huynh-Dinh, T.; Genissel, B.; Langlois d'Estaintot, B.; Igolen, J. *Biochemistry* **1984**, *23*, 1362−1371.
(5) Sugiyama, H.; Kawai, K.; Matsunaga, A.; Fujimoto, K.; Saito, I.; Robinson, H.; Wang, A. H.-J. *Nucleic Acids Res.* **1996**, *24*, 1272−1278.
(6) Kawai, K.; Saito, I.; Sugiyama, H. *J. Am. Chem. Soc.* **1999**, *121*, 1391−1392.
(7) Oyoshi, T.; Kawai, K.; Sugiyama, H. *J. Am. Chem. Soc.* **2003**, *125*, 1526−1531.
(8) Xu, Y.; Ikeda, R.; Sugiyama, H. *J. Am. Chem. Soc.* **2003**, *125*, 13519−13524.
(9) Berova, N., Nakanishi, K., Woody, R. W., Eds. *Circular Dichroism: Principles and Applications*; Wiley-VCH: New York, 2000.
(10) Bauernschmitt, R.; Ahlrichs, R. *Chem. Phys. Lett.* **1996**, *256*, 454−464.
(11) Casida, M. E.; Jamorski, C.; Casida, K. C.; Salahub, D. R. *J. Chem. Phys.* **1998**, *108*, 4439−4449.
(12) Tsolakidis, A.; Kaxiras, E. *J. Phys. Chem. A* **2005**, *109*, 2373−2380.
(13) Varsano, D.; Di Felice, R.; Marques, M. A. L.; Rubio, A. *J. Phys. Chem. B* **2006**, *110*, 7129−7138.
(14) Nielsen, L. M.; Holm, A. I. S.; Varsano, D.; Kadhane, U.; Hoffmann, S. V.; Di Felice, R.; Rubio, A.; Nielsen, S. B. *J. Phys. Chem. B* **2009**, *113*, 9614−9619.
(15) Tonzani, S.; Schatz, G. C. *J. Am. Chem. Soc.* **2008**, *130*, 7607−7612.
(16) Casida, M. E.; Salahub, D. R. *J. Chem. Phys.* **2000**, *113*, 8918−8935.
(17) Dreuw, A.; Weisman, J. L.; Head-Gordon, M. *J. Chem. Phys.* **2003**, *119*, 2943−2946.
(18) Maitra, N. T.; Zhang, F.; Cave, R. J.; Burke, K. *J. Chem. Phys.* **2004**, *120*, 5932−5937.
(19) McCann, D. M.; Stephens, P. J. *J. Org. Chem.* **2006**, *71*, 6074−6098.
(20) Casida, M. E. *J. Mol. Struct.* **2009**, *914*, 3−18.
(21) Niehaus, T. A. *J. Mol. Struct.* **2009**, *914*, 38−49.
(22) Tawada, Y.; Tsuneda, T.; Yanagisawa, S.; Yanai, T.; Hirao, K. *J. Chem. Phys.* **2004**, *120*, 8425−8433.
(23) Chiba, M.; Tsuneda, T.; Hirao, K. *J. Chem. Phys.* **2006**, *124*, 144106-1-11.
(24) Nakatsuji, H.; Hirao, K. *J. Chem. Phys.* **1978**, *68*, 2053−2065.
(25) Nakatsuji, H. *Chem. Phys. Lett.* **1978**, *59*, 362−364.
(26) Nakatsuji, H. *Chem. Phys. Lett.* **1979**, *67*, 329−333.
(27) Nakatsuji, H. *Chem. Phys. Lett.* **1979**, *67*, 334−342.
(28) Nakatsuji, H. *Bull. Chem. Soc. Jpn.* **2005**, *78*, 1705−1724.
(29) Ehara, M.; Hasegawa, J.; Nakatsuji, H. SAC-CI Method Applied to Molecular Spectroscopy. In *Theory and Applications of Computational Chemistry: The First 40 Years, A Vol. of Technical and Historical Perspectives*; Dykstra, C. E., Frenking, G., Kim, K. S., Scuseria, G. E., Eds.; Elsevier: Oxford, U.K., 2005; pp 1099−1141.
(30) Miyahara, T.; Hasegawa, J.; Nakatsuji, H. *Bull. Chem. Soc. Jpn.* **2009**, *82*, 1215−1226.
(31) Bureekaew, S.; Hasegawa, J.; Nakatsuji, H. *Chem. Phys. Lett.* **2006**, *425*, 367−371.
(32) Nakatani, N.; Hasegawa, J.; Nakatsuji, H. *J. Am. Chem. Soc.* **2007**, *129*, 8756−8765.
(33) Fujimoto, K.; Hasegawa, J.; Nakatsuji, H. *Bull. Chem. Soc. Jpn.* **2009**, *82*, 1140−1148.
(34) Miyahara, T.; Nakatsuji, H. *Collect. Czech. Chem. Commun.* **2011**, *76*, 537−552.
(35) Sugiyama, H. Unpublished.
(36) Geertsen, J.; Rittby, M.; Bartlett, R. J. *Chem. Phys. Lett.* **1989**, *164*, 57−62.
(37) Stanton, J. F.; Bartlett, R. J. *J. Chem. Phys.* **1993**, *98*, 7029−7039.
(38) Ehara, M.; Ishida, M.; Toyota, K.; Nakatsuji, H. SAC-CI General-R Method: Theory and Applications to the Multi-Electron Processes. In *Reviews in Modern Quantum Chemistry (A Tribute to Professor Robert G. Parr)*; Sen, K. D., Ed.; World Scientific: Singapore, 2003; pp 293−319.
(39) SAC-CI GUIDE,. http:/www.qcri.or.jp/sacci/.
(40) Frisch, M. J.; Trucks, G. W.; Schlegel, H. B.; et al. *Gaussian 03*, development revision, revision E.05; Gaussian, Inc.: Wallingford, CT, 2004.
(41) Hohenberg, P.; Kohn, W. *Phys. Rev.* **1964**, *136*, B864−B871.
(42) Kohn, W.; Sham, L. J. *Phys. Rev.* **1965**, *140*, A1133−A1138.
(43) Salahub, D. R., Zerner, M. C., Eds. *The Challenge of d and f Electrons*; The American Chemical Society: Washington, D.C., 1989.
(44) Parr, R. G.; Yang, W.; *Density-Functional Theory of Atoms and Molecules*; Oxford University Press: Oxford, U.K., 1989.
(45) Becke, A. D. *J. Chem. Phys.* **1993**, *98*, 5648−5652.
(46) Lee, C.; Yang, W.; Parr, R. G. *Phys. Rev.* **1988**, *37*, 785−789.
(47) Hariharan, P. C.; Pople, J. A. *Theor. Chim. Acta* **1973**, *28*, 213−222.
(48) Francl, M. M.; Pietro, W. J.; Hehre, W. J.; Binkley, J. S.; DeFrees, D. J.; Pople, J. A.; Gordon, M. S. *J. Chem. Phys.* **1982**, *77*, 3654−3665.
(49) Tomasi, J.; Mennucci, B.; Cammi, R. *Chem. Rev.* **2005**, *105*, 2999−3093.
(50) Fukuda, R.; Ehara, M.; Nakatsuji, H.; Cammi, R. *J. Chem. Phys.* **2011**, *134*, 104109−1−11.
(51) Dunning, T. H., Jr.; Hay, P. J. In *Modern Theoretical Chemistry*; Schaefer, H. F., III., Ed.; Plenum: New York, 1976; Vol. 3, pp 1−28.
(52) Nakatsuji, H. *Chem. Phys.* **1983**, *75*, 425−441.
(53) Hocquet, A.; Leulliot, N.; Ghomi, M. *J. Phys. Chem. B* **2000**, *104*, 4560−4568.
(54) Mishra, S. K.; Mishra, P. C. *J. Comput. Chem.* **2002**, *23*, 530−540.
(55) Sprecher, C. A.; Johnson, W. C. *Biopolymers* **1977**, *16*, 2243−2264.
(56) Clark, L. B.; Peschel, G. G.; Tinoc, I., J.r *J. Phys. Chem.* **1965**, *69*, 3615−3618.
(57) Voet, D.; Gratzer, W. B.; Cox, R. A.; Doty, P. *Biopolymers* **1963**, *1*, 193−208.
(58) Hobza, P.; Mehlhorn, A.; Carsky, P.; Zahradnik, R. *J. Mol. Struct.* **1986**, *138*, 387−399.
(59) Hobza, P.; Šponer, J. *Chem. Rev.* **1999**, *99*, 3247−3276.